Journal of
Polymer Materials

Tech Science Press

Doi:10.32604/jpm.2025.064866

ARTICLE

Improvement of Surface Electrical Properties of Silicone Rubber Based on Fluorination

Hanbo Zheng, Yue Peng, Enpeng Qin and Yi Li*

Guangxi Key Laboratory of Power System Optimization and Energy Technology, Guangxi University, Nanning, 530004, China

*Corresponding Author: Yi Li. Email: yili665143@163.com

Received: 25 February 2025; Accepted: 05 June 2025; Published: 11 July 2025

ABSTRACT: Fluorination is a critical surface modification technique for enhancing the electrical performance of composite insulators. This study employs molecular simulations to examine the microstructure and space charge behavior of fluorinated and non-fluorinated silicone rubber under an electric field, with experimental validation. The results show that fluorinated silicone rubber exhibits lower total energy, higher polarization, and stronger dipole moments compared to its non-fluorinated counterpart, shifting the material from an insulating to a conductive state. Under lower electric field strengths, the carbon-silicon bonds in fluorinated silicone rubber are longer, but it maintains geometric stability under higher fields. The energy gap changes across different fluorination modes and varies with electric field strength, indicating that fluorination affects conductivity differently at various field intensities. Both fluorination methods improve conductivity in the 0–3.8 V/nm range, with substitutional fluorination showing superior performance between 3.8 and 8.9 V/nm. Above 9.1 V/nm, fluorination maximizes conductivity. The fluorinated samples exhibit a greater redshift at higher electric fields, resulting in enhanced conductivity and improved surface charge distribution. These findings offer insights into the microscopic effects of fluorination on silicone rubber's electrical properties, while experiments confirm that fluorination increases hydrophobicity and boosts DC flashover voltage, further enhancing the material's performance.

KEYWORDS: Fluorination; composite insulators; molecular simulation; silicone rubber; electrical properties

1 Introduction

Silicone rubber is a unique polymer material primarily composed of siloxane polymers. It possesses outstanding properties, including high hydrophobicity, electrical insulation, resistance to extreme temperatures, ozone aging, oil, radiation, and combustion. These characteristics make it widely used in various fields such as electronics, electrical appliances, instrumentation, aviation, aerospace, and defense. Silicone rubber's excellent resistance to high temperatures, dirt, and aging ensures that insulators perform optimally in environments with high contamination and temperature. Due to its exceptional physical and chemical properties, silicone rubber plays an indispensable role in insulation applications [1–4]. Insulators, as the main part of the external insulation, are very important for the reliable and safe operation of the power grid. 1950s: the composite insulators are born. With the development of the times, SIR (silicone rubber), with its excellent performance, such as small quality, low price, and suitability for the preparation of a variety of shapes, gradually replaced the ethylene-propylene rubber, polytetrafluoroethylene, and so on to become the main material of the composite insulators' umbrella skirt sheath.

There exists a certain potential difference between the two poles of the insulator, and the appearance of flashover and insulation breakdown is extremely harmful to the power system [5]. Practice has shown that the flashover voltage along the solid-gas interface of insulators is much lower than the breakdown voltage of the solid medium and the breakdown voltage of the pure air gap, so the actual insulating performance of insulators often depends on the flashover [6]. The flashover voltage is related to the electric field distribution, the roughness of the insulator surface, the material dielectric constant, and other factors. The accumulation and dissipation of surface charge of the insulator can also have an effect on the flashover properties [7]. The accumulated surface charge causes electric field distortion and also provides seed charge for the development of flashover, which will result in a decrease in the flashover voltage. Surface charge buildup on insulators subjected to high voltage direct current (DC) fields can be more severe than in alternating current (AC) fields [8]. For cable and gas-insulated systems, some scholars have conducted many studies on the charge accumulation on insulators and its effect on the flashover by applying coatings on the insulator surface or chemical modification to increase the surface conductivity and inhibit the charge accumulation on the surface to improve the flashover voltage of insulators. In fact, the phenomenon of charge accumulation on the surface of insulating materials is a key factor affecting the flashover [9–11].

Insulator flashover along the surface is a gas discharge phenomenon that occurs at the gas-solid interface. Along-face flashover occurring in a vacuum is related to the electrode structure, applied electric field, surface condition of the dielectric, uniformity of the insulating material, etc. Gao et al. [12] introduced charges to the surface of a sample using a pair of finger electrodes and then performed a DC flashover test to examine the changes in surface charge distribution before and after the flashover. The experimental results showed that introducing surface charge reduced the flashover voltage on the specimen compared to uncharged epoxy resin samples, and a significant amount of charge accumulated on the surface during the ramp-up phase of the DC flashover test. Nano-coatings for gas insulated switchgear (GIS) tubular insulators, as reported in the literature [13], have been developed to effectively prevent surface charge accumulation and improve the electric field distribution of insulators under both DC and AC voltages. These coatings can inhibit surface charge buildup by up to 51.2% under DC voltage and 9.3% under AC voltage. Xie et al. [14] conducted an experimental study on the charge accumulation and dissipation characteristics on the surface of insulating materials and their impact on DC flashover. The study found that surface charge affects flashover characteristics by influencing the surface electric field strength and the development of surface discharges. Surface charge buildup on insulating materials distorts the electric field distribution on the insulator surface, which can easily lead to flashover along the surface. This phenomenon is one of the most critical factors influencing the insulating performance of insulators. Compared to AC power transmission, DC power transmission, with its unidirectional and stable electric field, exacerbates surface charge accumulation. Consequently, studying the accumulation and dissipation of charge on insulating materials' surfaces becomes especially important. From this perspective, increasing the surface conductivity of silicone rubber can prevent surface charge accumulation, which should improve the flashover voltage of the silicone rubber.

In the past few years, numerous researchers have made efforts to treat silicone rubber through surface modification techniques, with the anticipation of enhancing the surface properties of SIR [15,16]. The commonly used surface modification techniques mainly include surface coating, plasma treatment, and fluorination treatment. The research group led by Prof. Zhenlian An from Tongji University discovered that the fluorinated surface layer generated by directly fluorinating polymeric materials like polyethylene (PE), polypropylene (PP), epoxy resin, and silicone rubber can effectively enhance the surface electrical properties of these materials [17–20]. Direct fluorination means that F_2 or F_2/N_2 reacts with polymers under specific environmental conditions, resulting in the formation of a compact fluorinated layer on the polymer surface.

This layer endows the polymer with surface properties similar to those of fluorinated polymers. When directly fluorinating silicone rubber, due to the highly reactive chemical properties of fluorine atoms in F_2, they are likely to undergo substitution or addition reactions with the groups in the silicone rubber. It has been investigated by many studies to enhance the surface conductivity of silicone rubber through fluorination to improve the along-surface flash performance of silicone rubber in the expectation of effectively reducing the fouling flash accidents of silicone rubber in practical applications. However, at present, the microscopic mechanism of fluorination on the surface of silicone rubber to improve the surface charge distribution has not been clarified, and no study has been conducted to investigate the effect of fluorination on the surface electrical properties of silicone rubber by means of quantum chemistry.

In order to study the influence of fluorination on the electrical aging properties of silicone rubber, this study employs quantum chemical methods for theoretical investigation. In this study, Gaussian 09W software was used to construct and optimize the model of silicone rubber moleculars before and after fluorination based on a semi-empirical method. Subsequently, the front orbitals of the silicone rubber molecules were analyzed by Lu and Chen [21] software to determine the internal active reaction sites, and the changes in the microscopic internal structures, system energies, molecular dipole moments, and molecular polarizabilities of the silicone rubber molecules before and after the fluorination under different conditions of the applied electric field were studied in depth and analyzed comprehensively. After that, by analyzing the infrared spectra and space charge characteristics of the silicone rubber molecules before and after fluorination, the effect of fluorination on the improved surface charge distribution of silicone rubber in the presence of an electric field is revealed. Finally, the improvement effect of fluorination on the surface conductivity of silicone rubber was demonstrated by measuring the surface conductivity of silicone rubber before and after fluorination.

2 Semi-Empirical Method and Model Building

2.1 Semi-Empirical Method

The semi-empirical approach is a quantum-mechanical calculation method that has been simplified. By introducing empirical parameters, it enables the rapid calculation of the electronic structure of relatively large molecules. This method finds its main applications in organic chemistry, inorganic chemistry, and materials science to predict various molecular properties such as geometric configurations, vibrational frequencies, and electronic spectra [22,23]. In the realm of high-voltage DC insulation, this method offers a more efficient way to investigate the microscopic phenomena of insulating materials.

To study the molecular structure of silicone rubber, taking into account the influence of external electric fields on the molecular structure, this paper adopts a semi-empirical method and incorporates the field intensity as a potential energy term in the equation. When no external electric field is present, the corresponding Hamiltonian is H_0. Once an electric field is applied, the Hamiltonian of the SIR molecular system, H, can be expressed as shown in Eq. (1). H_{int} stands for the Hamiltonian when an external electric field acts on the molecular system. Based on the dipole approximation, when interacting with the silicone rubber molecular system, the effect caused by the electric field can be represented by Eq. (2), where μ symbolizes the electric dipole moment of the molecule and F indicates the intensity of the electric field. The entire calculation was done using the Gaussian09W software package; further analyses were performed using Multiwfn 3.7 [24] software and VMD 1.9.3 [25] software.

$$H = H_0 + H_{\text{int}} \tag{1}$$

$$H_{\text{int}} = -\mu \times F \tag{2}$$

2.2 Model Building

The main chain of silicone rubber consists of oxygen and silicon atoms alternately, with two methyl groups attached to the silicon atom, and the molecular structural formula is shown in Fig. 1. Since silicone rubber moleculars are very large, it is impractical to perform simulations of real materials at different electric field intensities. The silicone rubber selected in this study is methyl vinyl silicone rubber, which is mainly composed of dimethylsiloxane chains and methyl vinyl silicone chains, as can be seen by the molecular structural formula in Fig. 1. The polymer is a long-chain molecule formed by the monomer molecules through the polymerization reaction. If the polymerization is too high, just increase the number of server calculations, and the polymer in the electric field does not produce a relatively large difference with the change of the degree of polymerization. On the other hand, the physical property and chemical property of the polymer depend largely on the structure and properties of the monomer molecules [10]. Since both structures, dimethylsiloxane chains and methyl vinylsiloxane chains, are recurring in silicone rubber, so as to balance the efficiency of the computational simulation and the reliability of the results, the molecular model is established to model the polymerization degree of 3 (i.e., m = 3) for dimethylsiloxane chains and 1 (i.e., n = 1) for methyl vinylsiloxane chains.

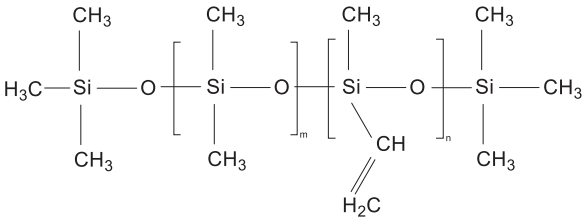

Figure 1: The molecular structure of SIR molecules [26]

So as to understand the effect of the electric field on the weak locations of the polymer, models with different values of polymerization degree were selected for pre-simulation in this study, and the degree of polymerization had little effect on the results. Considering that there is no need to use molecular models with thousands of degrees of polymerization, this paper constructs a molecular model of the silicone rubber monomer, shown in Fig. 2, with the aim of investigating its microscopic mechanism under the action of an electric field.

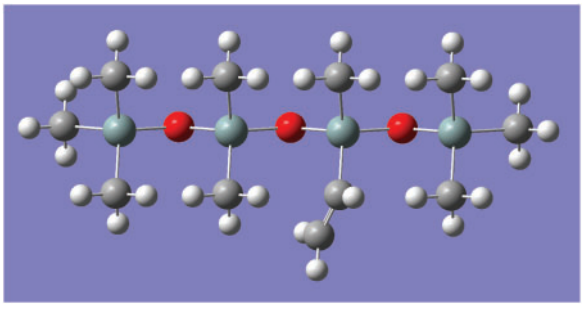

Figure 2: The molecular model of SIR molecules

The different positions of fluorine atoms in the fluorinated silicone rubber have different effects on the change trend of silicone rubber under an electric field. At present, the microscopic mechanism of the fluorination reaction of silicone rubber has not been clarified, and two models of fluorination of silicone rubber were established in this study. In the first model, the fluorine atom has a substitution reaction with the silicone rubber, the F atom replaces the H atom on the methyl group in the silicone rubber, and the molecular structure formula is shown in Fig. 3a, and the model of this fluorinated silicone rubber is shown in Fig. 4a, which is hereinafter referred to as the molecular model of the silicone rubber as E1; in the second model, the fluorine atom has an addition reaction with the vinyl group in the SIR, and the molecular structure formula is shown in Fig. 3b, the model of such fluorinated silicone rubber is constructed as shown in Fig. 4b, which is referred to as E2; and the molecular model of unfluorinated SIR, which is referred to as E.

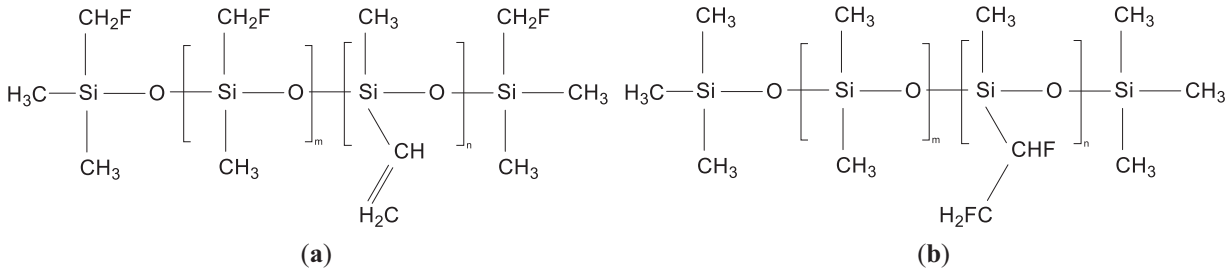

Figure 3: The molecular structure of fluorinated SIR molecules: (**a**) Molecular structure of SIR undergoing substitution fluorination reaction; (**b**) Molecular structure of SIR undergoing addition fluorination reaction

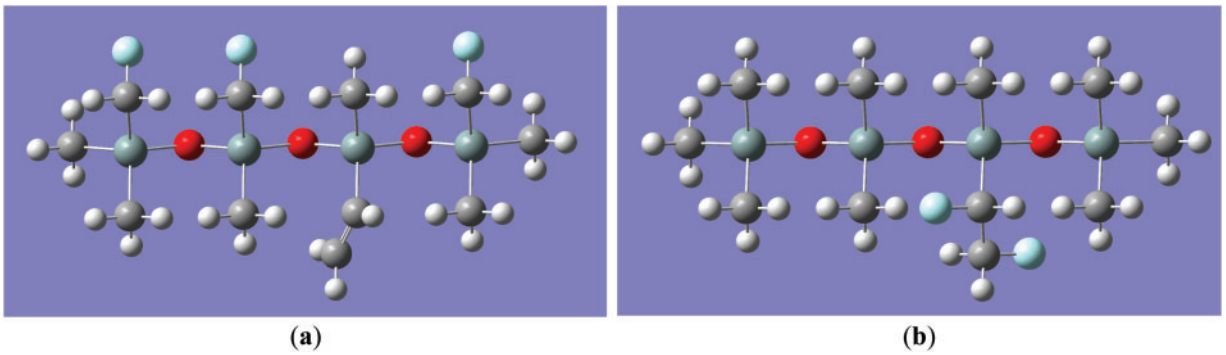

Figure 4: The molecular model of fluorinated SIR molecules: (**a**) The molecular model of SIR undergoing substitution fluorination reaction; (**b**) The molecular model of SIR undergoing addition fluorination reaction

In this study, the simulation of silicone rubber monomer molecules before and after fluorination is carried out by quantum chemical methods, which can obtain key information such as the electronic structure, reactivity, and energy state of silicone rubber monomer molecules before and after fluorination. The specific steps are as follows: Firstly, the semi-empirical PM3-based method is used to optimize the geometrical configurations of the initial molecular model of silicone rubber as well as the two fluorination molecular models of silicone rubber to obtain a state of the lowest energy. After setting the relevant calculation parameters, the keyword "field" is increased, and the electric field intensity is gradually increased from 0, which rises at a step voltage of every 5.142×10^{-2} V/nm. Since the process of simulation calculation is of short duration and the electric field is of long duration, the time effect is counteracted by using the addition of different electric field intensities, so the field intensities set in this study are far beyond the breakdown field

intensities of the silicone rubber in order to research the microscopic mechanism of the change in surface electrical properties of silicone rubber before and after fluorination.

3 Experiment

3.1 Sample Preparation and Fluoridation

For the preparation of the silicone rubber specimens, POWERSIL® 737 from WACKER, Germany, was used as the raw material. Component A is a vinyl-terminated polydimethylsiloxane (with platinum catalyst): viscosity (25°C, same below) 10 Pa·s, vinyl mass fraction 0.12%, platinum catalyst: Pt content 5×10^{-3}. Component B is a hydrogenated silicone oil: viscosity 20 mPa·s, active hydrogen mass fraction 0.6%. Components A (containing the platinum catalyst) and B (containing the crosslinker) were weighed and mixed in a 1:1 ratio for 2 h. After that, the moldboard was filled, and the vulcanization process was carried out, setting the vulcanization conditions as pressure 20 MPa, temperature 105°C, and duration 20 min [27–29]. After unloading the mold, the 2 mm thickness of the vulcanized silicone rubber sheet samples, the samples will be cut into 7.5 cm × 7.5 cm size and placed into the laboratory set up in the fluoride treatment system using a fluorine gas concentration of 12.5% of the F_2/N_2 gas mixture for fluoride treatment. The fluoride durations are 1 h. This paper will not be fluoridated specimens called. In this paper, the unfluoridated specimen is referred to as sample V, and the fluoridated specimens are referred to as sample F1.

3.2 Attenuated Total Reflection Infrared Spectroscopy (ATR-IR), X-Ray Photoelectron Spectroscopy (XPS) and Contact Angle Measurement

Attenuated Total Reflection Infrared Spectroscopy (ATR-IR) can detect the changes in the surface layer of the sample after fluoridation, determine the chemical composition and molecular structure of the fluoride layer, and analyze the reaction mechanism between fluorine gas and the silicone rubber samples in the process of fluoridation. In this paper, a Thermo Nicolet NEXUS 670 Fourier (Thermo Fisher Scientific, Waltham, MA, USA) infrared spectrometer was used to detect the silicone rubber samples.

X-ray Photoelectron Spectroscopy (XPS) is a surface composition analysis technique, with a probing depth of approximately a few nanometers into the sample surface, which is shallower than the analysis depth of ATR-IR. In this study, tests were conducted using a Thermo Scientific XPS system (Thermo Fisher Scientific, Waltham, MA, USA), with an Al K-Alpha X-ray source.

Wettability reflects the ability of a liquid to spread on a solid surface. The wettability of a solid surface is the macroscopic external manifestation of the surface energy of the solid material. In this study, the static contact angle of a liquid on the material surface will be measured using the sessile drop method to evaluate the surface wettability of the silicone rubber samples. The experimental instrument used is the JC2000C contact angle meter, manufactured by Shanghai Zhongchen Digital Technology Equipment Co., Ltd. (Shanghai, China).

3.3 Surface Conductivity Measurement

In this paper, the value of surface conductivity is calculated from the measured surface resistivity. The instrument used is the ZC-90G High Insulation Resistance Measuring Instrument produced by Shanghai Tai-O Electronics Co. (Shanghai, China). In the experimental process, the use of a "three-electrodes" structure, with reference to the national standard GB1410-89 using the measurement device shown in Fig. 5 for measurement.

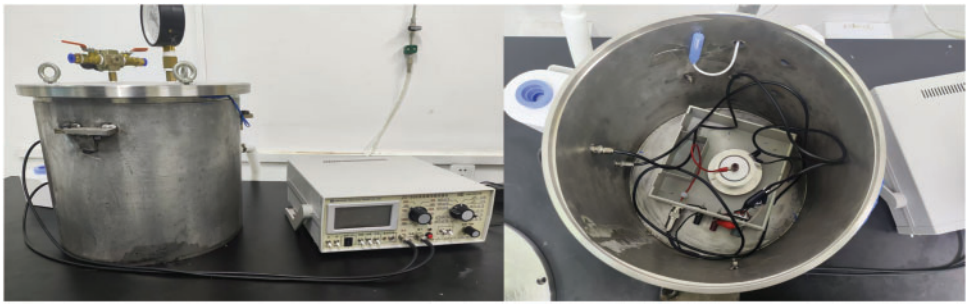

Figure 5: Surface conductivity testing device

3.4 DC Surface Flashover Test

The equipment used for the DC surface flashover test was a power frequency withstand voltage test system produced by Huagao Electric (Hubei) Co., Ltd. (Wuhan, China). The high-voltage DC power source was controlled by an integrated voltage regulation control cabinet, which set the DC step-up voltage mode. The voltage was first increased at a rate of 1.6 kV/s to −14 kV, and then each voltage step was increased by 0.5 kV. The duration of each voltage step was set to 10 min, until surface flashover occurred on the specimen. In this study, the flashover voltage for seven sets of original and fluorinated specimens was measured, and the average value was taken for analysis. The basic parameters and operating conditions of ZC-90G are shown in Table 1 below.

Table 1: Basic parameters and operating conditions of ZC-90G

Basic parameters and operating conditions	Data
Resistance measurement range	0–2×10^{17} Ω
Current measurement range	10^{-16}–2×10^{-4} Ω
Rated voltage	10, 25, 50, 100, 250, 500, 1000 V
Measurement timing	1–7 min
Temperature	0–40°C
Humidity	≤80%
Power supply	DC 8.5–12.5 kV

4 Simulation Results and Analysis

4.1 Effect of External Electric Field on Molecular Structure after Fluorination

Under the influence of the external electric field, the chemical bond lengths in the molecules change accordingly, thus characterizing the change in the molecular geometry under the influence of the electric field. In the molecular system, the positive and negative charges are affected by the external electric field, generating a mutual transfer effect, which causes a certain degree of stretching of the SIR molecular chain, thereby reducing the stability of the internal geometric structure.

The molecular chain of silicone rubber changes dynamically within electric fields of different intensities, as can be seen in Fig. 6 (In the molecular model E1, the fluorine atoms undergo a substitution reaction with the silicone rubber; in the molecular model E2, the fluorine atoms undergo an addition reaction with the vinyl groups in the silicone rubber; the molecular model of the unfluorinated silicone rubber is referred

to as E), in which the direction of molecular chain extension is consistent with the applied electric field's direction. Before fluorination, the C40-Si11 bond length of the silicone rubber molecule is stretched with the enhancement of the electric field intensity. After fluorination, for both structures, when the electric field strength is lower, the C40-Si11 bond length of the silicone rubber molecules is longer than that of the unfluorinated silicone rubber. However, the change with respect to the electric field strength is not significant. This suggests that, under lower electric field strengths, the electrical properties of fluorinated silicone rubber are less stable than those of the unfluorinated material. In this state, free radicals that can move more easily within the silicone rubber are more likely to form. The macroscopic result is an increase in surface conductivity, which aids in improving the charge distribution on the material's surface, ultimately enhancing its surface flashover performance.

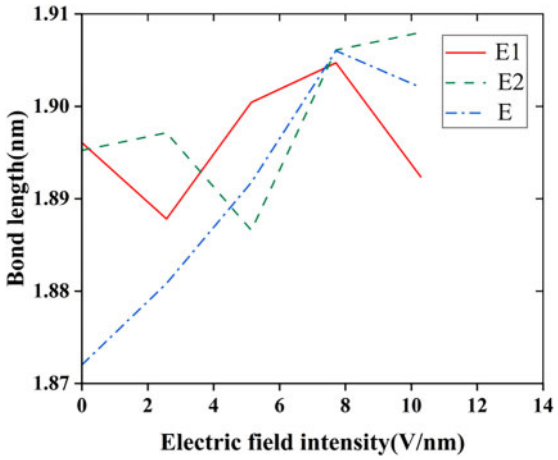

Figure 6: The change in bond length of SIR molecules before and after fluorination

4.2 Effect of External Electric Field on Total Molecular Energy, Dipole Moment, and Polarizability after Fluorination

The polar moment and polarizability can characterize the spatial configuration and molecular polarity of the molecules to an extent. When the external electric field strength is gradually increased, the energies of the three silicone rubber molecules before and after fluoridation are both gradually decreased, in which the energy of the two SIR models after fluoridation is smaller than that of the unfluoridated silicone rubber model, as shown in Fig. 7 (In the molecular model E1, the fluorine atoms undergo a substitution reaction with the silicone rubber; in the molecular model E2, the fluorine atoms undergo an addition reaction with the vinyl groups in the silicone rubber; the molecular model of the unfluorinated silicone rubber is referred to as E). The transfer of electrons along the direction of the electric field makes the charge of each atom in the direction of the electric field larger, which increases the silicone rubber molecule electric dipole moment u. From Eq. (2), it can be seen that, with the increase of the electric field strength, the absolute value of the interaction energy between the electric field and the molecule, H_{int}, increases, and the interaction energy is negative, which leads to the decrease of the energy H of the molecular system. The energy of the two types of silicone rubber molecules after fluoridation is overall less than that of the unfluoridated silicone rubber molecules. This is due to the fact that the fluoridated silicone rubber molecules form C-F bonds with greater bonding energy, which makes the silicone rubber molecules have a very large release of energy, and thus the silicone rubber molecules have a lower energy level, and the entire molecule is more stable than it was before.

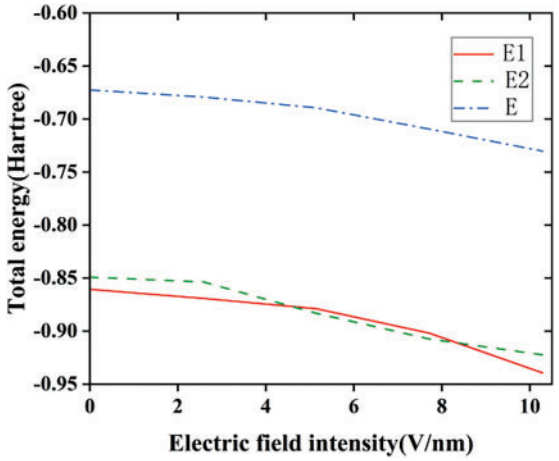

Figure 7: The variation of SIR molecular total energy before and after fluorination

The increase in the charge of each atom is accompanied by the generation of a larger polarizability and dipole moment in the silicone rubber molecule, as shown in Figs. 8 and 9 (In the molecular model E1, the fluorine atoms undergo a substitution reaction with the silicone rubber; in the molecular model E2, the fluorine atoms undergo an addition reaction with the vinyl groups in the silicone rubber; the molecular model of the unfluorinated silicone rubber is referred to as E). As the molecule is confined by its size, the electrons under the electric field are gradually unbound from the nuclei of the atoms and are moved under the effect of the continuous electric field towards a position in the direction opposite to that of the applied electric field, which results in an ever-increasing dipole moment of the molecule. Under the electric field, the dipole of the molecule will undergo directional rotation, which leads to the formation of an equivalent polarized space charge inside the dielectric. As the electric field strength adds, the polarizability increases accordingly, which in turn leads to an increase in the polarized space charge density. When the external electric field exceeds the threshold of the dipole moment, the dipole moment surpasses its critical value, causing electrons to detach from the nucleus and form free electrons, thereby increasing the surface conductivity of the material. Furthermore, the polarity of fluorinated silicone rubber molecules is higher than that of unfluorinated silicone rubber molecules, making them more reactive. As a result, under the prolonged influence of the external electric field, the internal molecular chain system of fluorinated silicone rubber becomes more unstable compared to the unfluorinated counterpart. This instability facilitates the formation of free radicals, which further enhances the surface conductivity of the material. Additionally, this promotes a more favorable charge distribution on the surface of the silicone rubber, ultimately improving its surface flashover performance.

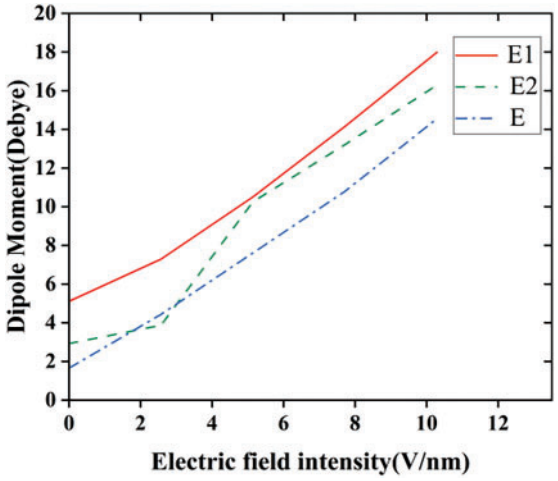

Figure 8: The variation of SIR molecular dipole moment before and after fluorination

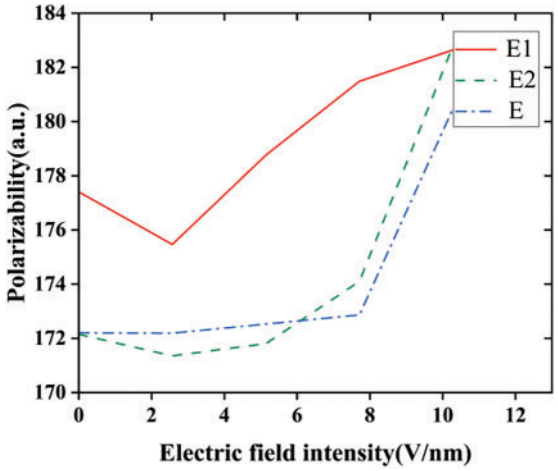

Figure 9: The variation of SIR molecular polarizability before and after fluorination

4.3 Effect of External Electric Field on Molecular Front Orbitals after Fluorination

The electronic kinematic properties of silicone rubber within different external electric fields are investigated by means of energy gaps (Eg), the front orbital energy levels, and orbital compositions. Figs. 10 and 11 show the results of energy levels and Eg calculations. In this definition, Eg represents the energy level difference between the lowest unoccupied molecular orbital (LUMO) and the highest occupied molecular orbital (HOMO). According to frontier orbital theory, HOMO orbitals with higher electron energies are less bound and are more prone to electron leaps, whereas LUMO orbitals with lower energies are more receptive to electrons [30]. In general, the lower the energy gap, the higher the conductivity of the material, and from Fig. 10, it shows that diverse fluorination methods have different effects on the conductivity of SIR at diverse electric field intensities.

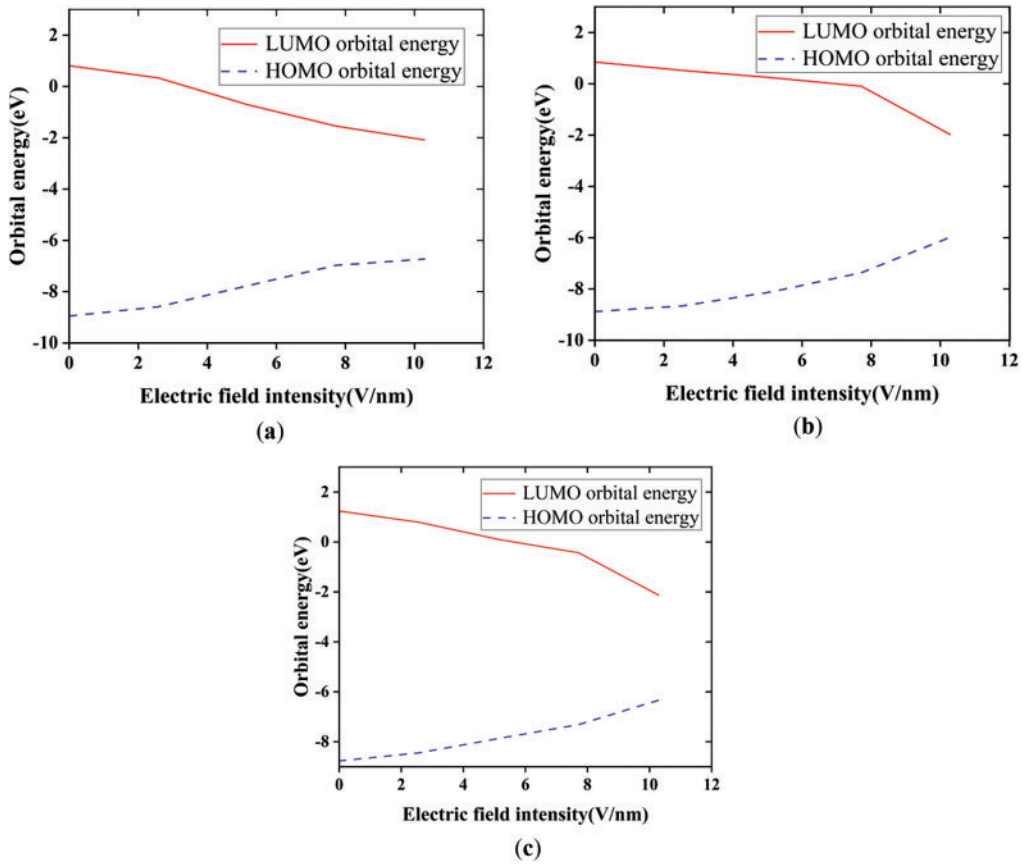

Figure 10: Changes in orbital energy levels of SIR before and after fluorination at different electric fields: (**a**) Changes in orbital energy levels of SIR undergoing substitution fluorination reaction at different electric fields; (**b**) Changes in orbital energy levels of SIR undergoing addition fluorination reaction at different electric fields; (**c**) Changes in orbital energy levels of unfluorinated SIR at different electric fields

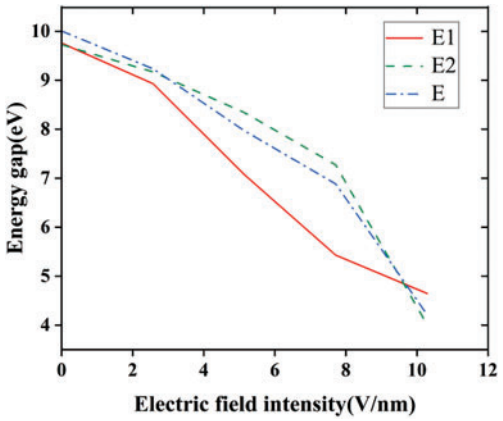

Figure 11: The variation in energy gaps at different electric fields before and after fluorination

The results show that the two fluorination methods have distinct effects on the conductivity of silicone rubber at different electric field strengths (Fluorination Method I refers to the fluorination process in which

fluorine atoms undergo a substitution reaction with silicone rubber, while Fluorination Method II refers to the fluorination process in which fluorine atoms undergo an addition reaction with silicone rubber). In the electric field strength range of 0–3.8 V/nm, both fluorination methods enhance the conductivity of silicone rubber. Between 3.8 and 8.9 V/nm, Fluorination Method I increases conductivity, while Fluorination Method II decreases it. In the range of 8.9–9.1 V/nm, both fluorination methods improve the conductivity. However, at electric field strengths greater than 9.1 V/nm, the effects of the two methods diverge: Fluorination Method II increases conductivity, whereas Fluorination Method I reduces it. The increase in surface conductivity helps improve the surface charge distribution, thereby enhancing the surface flashover performance of the silicone rubber. Based on these findings, the choice of fluorination method for silicone rubber can be tailored according to the electric field strength of the application environment.

The microscopic mechanism of space charge changes in SIR under the effect of the external electric field is investigated using orbital cloud diagrams. Fig. 12 shows the frontline orbital cloud diagrams of 3 kinds of silicone rubber molecules at electric field intensities of 0 and 10.3 V/nm, which can reflect the motion characteristics of space charge. According to the frontline orbital maps, the orbital distributions of the three molecular models are similar, with the HOMO orbitals uniformly distributed in the molecular before the application of the electric field, while the LUMO orbitals are mainly aggregated at the right-hand side of the molecular. However, the effect of the external electric field led to significant changes in the front orbitals and the molecular active reaction sites. When the electric field gets to 10.3 V/nm, the LUMO orbitals mainly move to the left-hand side of the molecular, and the HOMO orbitals move to the right-hand side of the molecular, and the change of the energy level distribution produces an obvious difference between the left and right sides of the molecular chain, causing them to exhibit different electrophilicity and nucleophilicity. This implies that the applied electric field gradually raises the HOMO energy level and lowers the LUMO energy level, which changes the characteristics of the reactive sites of the silicone rubber molecules. In the meantime, the energy levels of the LUMO and HOMO orbitals are close to each other. The Eg between the LUMO orbitals and HOMO orbitals of the three materials are 4.65, 4.01, and 4.22 eV, respectively. Therefore, at the electric field strength of 10.3 V/nm, the surface conductivity of the additively fluorinated silicone rubber increases as electrons are more likely to travel freely between the valence band and the conduction band than those of the unfluoridated SIR material. In the case of substitutional fluorination, the electrons are less likely to travel freely between the valence and conduction bands, and the surface conductivity decreases compared to unfluorinated silicone rubber. This result aligns with the conclusion drawn from the energy gap analysis, which suggests that at high field strengths, the addition-type fluorination enhances the conductivity of silicone rubber, while the substitution-type fluorination reduces its conductivity.

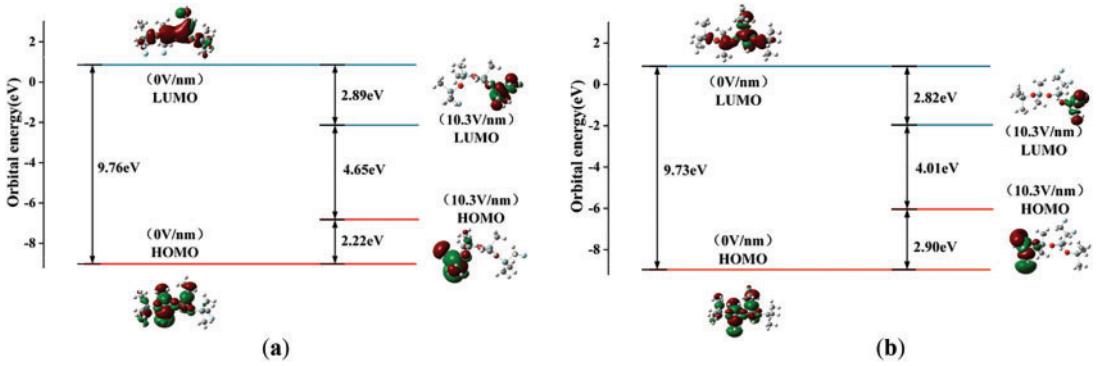

Figure 12: (Continued)

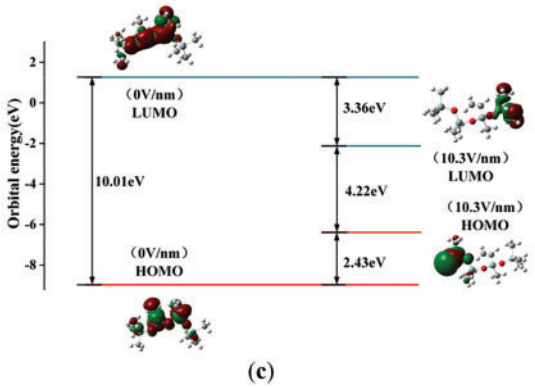

Figure 12: The molecular orbital of SIR molecules before and after fluorination: (a) The molecular orbital of SIR molecules undergoing substitution fluorination reaction; (b) The molecular orbital of SIR molecules undergoing addition fluorination reaction; (c) The molecular orbital of unfluorinated SIR molecules

4.4 Effect of External Electric Field on Infrared Spectra after Fluorination

The calculated results were further processed using Multiwfn software to obtain the infrared spectral data of E1, E2, and E at external electric field intensities of 0, 2.571, 5.142, 7.713, and 10.284 V/nm, respectively, which are presented in Fig. 13. The overall shift of the IR spectra in the direction of decreasing frequency is called redshift, indicating a decrease in chemical bonding energy, while the shift in the direction of increasing frequency is called blueshift, indicating an increase in chemical bonding energy. From Fig. 13, it shows that with the increase of the external electric field, the absorption peaks of the IR spectra of the three silicone rubber molecular models up to 2000 cm^{-1} appeared to be shifted in the direction of decreasing frequency as a whole, and under the effect of an external electric field, the bond lengths of the corresponding chemical bonds were elongated, which led to a decrease in the chemical bonding energy. Further analysis from Fig. 13, the magnitude of the red shift in the infrared spectrum of the unfluorinated specimen E is relatively small within the field intensity of 7.713 V/nm, and the magnitude of the red shift in the infrared spectrum is relatively large when the electric field strength exceeds 7.713 V/nm, which proves that at electric field intensities greater than 7.713 V/nm, the internal molecular structure of unfluorinated silicone rubber becomes unstable and the conductivity becomes greater. For the fluorinated silicone rubber model E1, the magnitude change of the red shift of the infrared spectrum is relatively small within the field intensity of 5.142 V/nm; when the electric field intensity exceeds 5.142 V/nm, the magnitude change of the red shift is relatively large, which proves that at electric field strength greater than 5.142 V/nm, the internal molecular structure of fluorinated silicone rubber model E1 becomes unstable and the conductivity becomes greater. For the fluorinated silicone rubber model E2, the magnitude change of the red shift of the infrared spectrum is relatively small within the field intensity of 7.713 V/nm; when the electric field strength exceeds 7.713 V/nm, the magnitude change of the red shift is relatively large, which proves that at electric field intensities greater than 7.713 V/nm, the internal molecular structure of fluorinated silicone rubber model E2 becomes unstable and the conductivity becomes greater. At higher electric field strengths, the red shift observed in the infrared spectrum of the fluorinated silicone rubber model E2 is significantly greater than that in both the unfluorinated silicone rubber model and the fluorinated silicone rubber model E1. This indicates that the internal structure of the fluorinated silicone rubber model E2 is more prone to free radical formation compared to both the unfluorinated model and the E1 model. As a result, at higher electric field strengths, the number of free radicals generated in E2 is higher than in E1 or the unfluorinated model, leading to increased electrical conductivity. Consequently, the flashover performance along the surface of the silicone rubber material is enhanced.

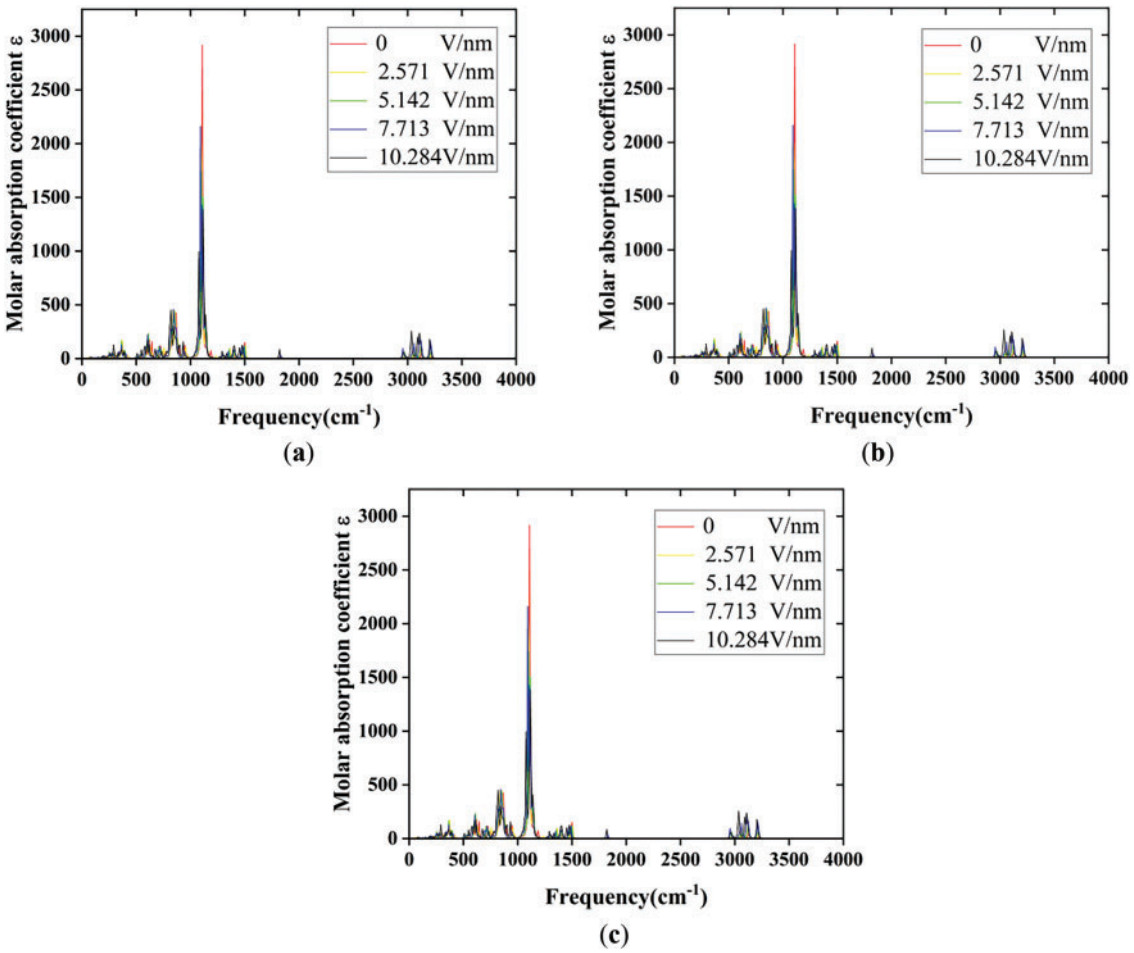

Figure 13: The infrared spectrum of SIR molecules before and after fluorination: (**a**) The infrared spectrum of SIR molecules undergoing substitution fluorination reaction; (**b**) The infrared spectrum of SIR molecules undergoing addition fluorination reaction; (**c**) The infrared spectrum of unfluorinated SIR molecules

4.5 ATR-IR, XPS and Contact Angles before and after Fluorination

The samples of silicone rubber before and after fluorination were analyzed using Attenuated Total Reflectance Infrared Spectroscopy (ATR-IR) to examine their molecular structure and chemical composition. In Fig. 14, (a) represents the infrared absorption spectrum of the unfluorinated sample, while (b) corresponds to the infrared absorption spectra of samples F1.

By comparing the infrared absorption spectra of samples F1(b) with that of the unfluorinated sample (a), it can be observed that fluorination significantly reduces the intensity of several absorption peaks associated with -CH_3 in the silicone rubber samples. These changes are undoubtedly related to the substitution of other atoms or groups by fluorine atoms during the fluorination reaction. During the reaction, fluorine atoms may replace one or more hydrogen atoms in -CH_3, forming C-F bonds, which results in the weakening of the infrared absorption peaks related to -CH_3 in the spectrum.

Fig. 15a shows the high-resolution Si 2p XPS spectrum of the unfluorinated sample. After peak fitting, two characteristic peaks were observed at 102.2 and 103.7 eV, which correspond to Si-O_2C_2 and Si-O_4, respectively. Commercial silicone rubber products are typically considered to contain minimal particles, but the presence of the Si-O_4 characteristic peak indicates that the silicone rubber used in this study

actually contains a significant amount of SiO_2. Fig. 15b shows the high-resolution Si 2p XPS spectrum of the fluorinated sample F1. By comparing Fig. 15a,b, it can be observed that there are significant differences in the Si 2p spectra before and after fluorination. After fluorination, the Si 2p high-resolution spectrum of the sample shows four characteristic peaks. The peak fitting results for the fluorinated sample's Si 2p spectrum reveal the presence of four characteristic peaks: Si-O_2C_2, Si-O_2CF, Si-O_3F, and Si-O_2F_2. The Si-O_3F characteristic peak suggests that SiO_2 particles on the surface layer of the silicone rubber were also fluorinated during the fluorination process.

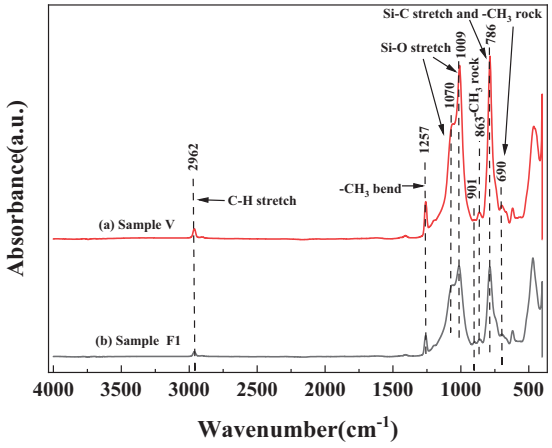

Figure 14: ATR-IR spectrum of unfluoridated and fluoridated samples

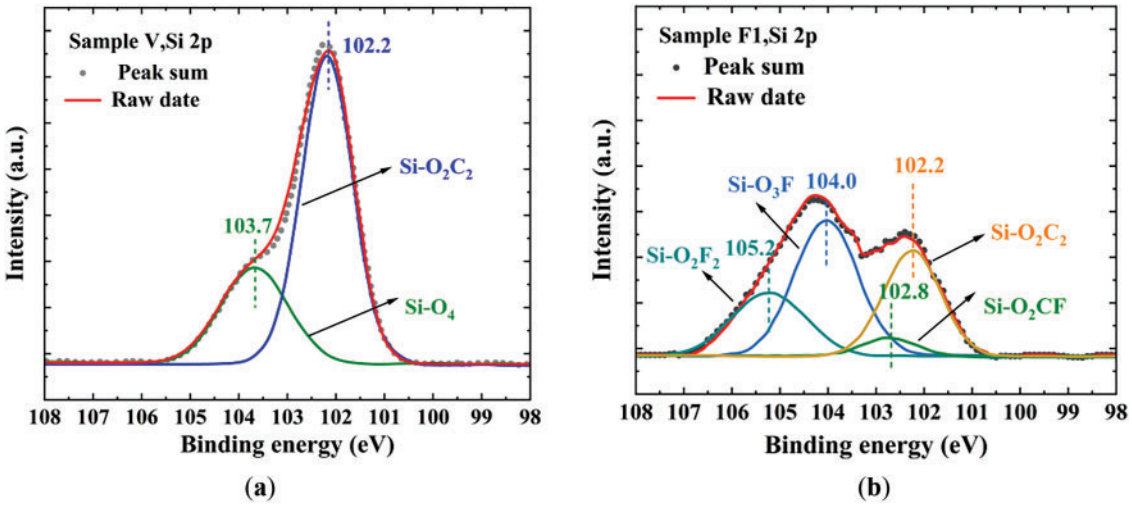

Figure 15: The XPS high-resolution spectra of unfluorinated and fluorinated samples: (**a**) The XPS high-resolution spectra of silicone rubber before fluorination; (**b**) The XPS high-resolution spectra of silicone rubber after fluorination

As shown in Fig. 16, the contact angle of water on silicone rubber increased from 106.97° to 148.06° after fluorination. Silicone rubber itself has high hydrophobicity, primarily due to the presence of a large number of methyl groups, which are non-polar. This makes the surface energy of silicone rubber relatively low, making it difficult to wet. After fluorination, the surface energy of the silicone rubber sample significantly decreased, and the static contact angle of water on the surface increased to 148.06°. During the fluorination reaction,

fluorine atoms enter the silicone rubber surface and introduce fluorine elements into the methyl groups on the surface. The formation of fluorinated methyl groups lowers the surface energy of the material, which is the reason why the hydrophobicity of the sample's surface is further enhanced after fluorination.

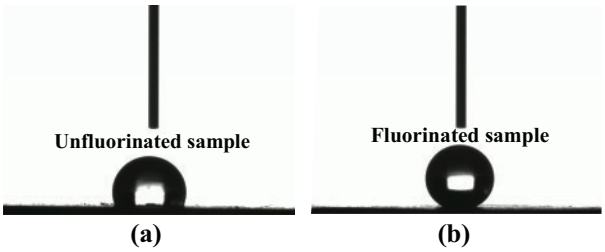

Figure 16: The contact angle of water on silicone rubber before and after fluorination: (**a**) The contact angle of water on silicone rubber before fluorination; (**b**) The contact angle of water on silicone rubber after fluorination

4.6 Surface Conductivity of Silicone Rubber before and after Fluorination

Surface conductivity measurements of the unfluoridated specimen and the fluoridated specimen were carried out using a three-electrode structure, and Table 2 illustrates the results of the surface conductivity measurements of the different specimens.

Table 2: Surface conductivity of silicone rubber samples before and after fluorination

Sample type	Surface conductivity
Sample V	6.9×10^{-18} S
Sample F1	4.9×10^{-16} S

The conductivity test of silicone rubber specimens using the three-electrode method was carried out in the absence of an electric field, and it can be seen from the Table 2 that in the absence of an electric field, the surface conductivity of fluorinated specimen has a significant increase compared with that of the unfluorinated specimens. This conclusion is consistent with the simulation results in the previous paper, and verifies the correctness of the previous conclusion that fluorination has an enhancement effect on the surface conductivity of silicone rubber materials under the condition of low electric field strength.

Regarding the increase in surface conductivity of fluorinated silicone rubber, we speculate that the polymer surface structure changes after fluorination, particularly due to the formation of C-F bonds. These changes introduce relatively shallow physical traps on the surface, promoting surface charge conduction. Therefore, the improvement in surface conductivity of silicone rubber can be attributed to these structural changes. Additionally, fluorination enhances the polarity of silicone rubber molecules, increasing the polarization space charge density. When the dipole moment exceeds a critical value, electrons detach from the nucleus to form free electrons, further enhancing the surface conductivity of the material.

4.7 DC Surface Flashover Performance of Silicone Rubber before and after Fluorination

To verify the enhancement effect of fluorination on the DC surface flashover performance of silicone rubber, the DC surface flashover voltage of silicone rubber before and after fluorination was measured. The measurement results are shown in Table 3.

Table 3: Flashover voltage of the original and fluorinated specimens

Specimen number	Flashover voltage (kV)	
	V	F1
1	19.55	21.69
2	17.63	23.58
3	17.74	23.54
4	16.07	23.67
5	18.51	21.95
6	17.49	25.32
7	14.87	21.38

Fig. 17 shows the cumulative probability distribution of the flashover voltage for the original and fluorinated specimens. Furthermore, this study calculates the Weibull distribution parameters V_0 and the average flashover voltage for both the original specimen V and the fluorinated specimen, as shown in Table 4.

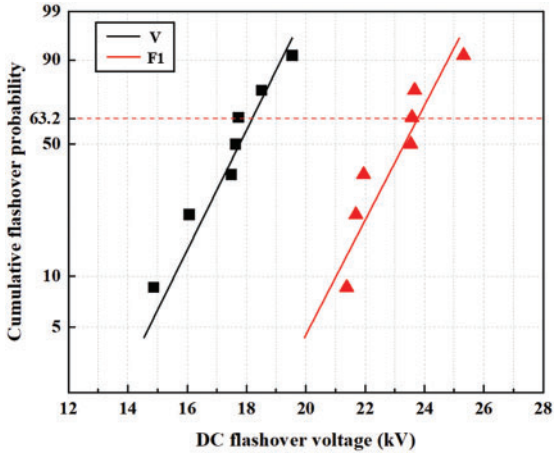

Figure 17: Weibull distribution of the flashover voltage for the original and fluorinated SIR

Table 4: Flashover voltage of the original and fluorinated specimens

Sample	Number of data	V_0 (kV) Weibull 63.2%	Average flashover voltage
	V	F1	F2
V	7	18.05	17.41
F1	7	23.65	23.02

From Table 4, it can be seen that after direct fluorination treatment, the breakdown voltage V_0 at a breakdown probability F(V) of 63.2% for the silicone rubber specimens increased from 18.05 kV for the original specimen to 23.65 kV for the fluorinated specimens F1. The average flashover voltage increased from 17.41 kV for the original specimen to 23.02 kV for the fluorinated specimens F1. Among them, the fluorinated specimen F1 exhibited the highest DC flashover voltage, with a voltage improvement rate of

32.22%. This confirms that fluorination has a significant enhancing effect on the flashover voltage of silicone rubber specimens.

5 Conclusion

In this study, the quantum chemical calculations of silicone rubber molecules before and after fluorination were carried out by a semi-empirical method, and experimental validation is used to reveal the changes in the chain structure and space charge properties of SIR molecules before and after fluorination under an electric field and to analyze the impact of fluorination on the electrical insulation properties of silicone rubber, and the following main results and conclusions can be drawn from this study:

Based on the quantum chemistry calculation results, fluorination increases the surface conductivity of silicone rubber, and the enhancement of surface conductivity helps improve the surface charge distribution, thereby increasing the surface flashover voltage of silicone rubber. Furthermore, the effect of different fluorination methods on the surface conductivity of silicone rubber varies under different electric field strengths: In the electric field strength range of 0–3.8 V/nm, both fluorination methods can increase the conductivity of silicone rubber; in the electric field strength range of 3.8–8.9 V/nm, substitutional fluorination can improve the conductivity of silicone rubber; in the electric field strength range of 8.9–9.1 V/nm, both fluorination methods can enhance the conductivity; while in the electric field strength range greater than 9.1 V/nm, addition-type fluorination is more effective in increasing the conductivity of silicone rubber. These results provide guidance for surface fluorination treatment of silicone rubber in different application scenarios.

Subsequently, a series of analyses including ATR-IR, XPS, and contact angle measurements were performed on both fluorinated and non-fluorinated silicone rubber samples to evaluate the impact of fluorination on their surface characteristics. The results from these experiments revealed that fluorination significantly alters the surface composition of silicone rubber, resulting in a notable increase in its hydrophobicity. This change in surface properties can be attributed to the incorporation of fluorine atoms, which modify the molecular structure and enhance the material's water-repellent nature. Additionally, without the application of an external electric field, the surface conductivity and DC flashover voltage of both fluorinated and non-fluorinated samples were measured. These measurements demonstrated that fluorination not only increases the surface conductivity of silicone rubber but also significantly improves its DC flashover voltage, thereby enhancing the material's overall electrical performance in non-electrically stressed conditions.

To gain a comprehensive understanding of the impact of fluorination on the properties of silicone rubber and to further expand on the findings of this study, we will conduct further research in the future using methods such as AFM, DSC, TGA/DTG, TEM, SEM, EDX/mapping, etc.

Acknowledgement: The authors extend gratitude to all individuals who contributed to the completion of this study.

Funding Statement: This work was supported in part by the National Natural Science Foundation of China under Grant 52277139 and 52367014, and in part by the Guangxi Science Fund for Distinguished Young Scholars under Grant 2024GXNSFFA999017.

Author Contributions: The authors confirm the contribution to the paper as follows: Conceptualization and data collation: Hanbo Zheng; formal analysis and writing: Yue Peng; project administration and draft manuscript preparation: Yi Li; software and validation: Enpeng Qin. All authors reviewed the results and approved the final version of the manuscript.

Availability of Data and Materials: The authors confirm that the data supporting the findings of this study are available within the article.

Ethics Approval: Not applicable.

Conflicts of Interest: The authors declare no conflicts of interest to report regarding the present study.

References

1. Liu PY, Li LC, Wang LM, Huang T, Yao YB, Xu WR. Effects of 2D boron nitride (BN) nanoplates filler on the thermal, electrical, mechanical and dielectric properties of high temperature vulcanized silicone rubber for composite insulators. J Alloys Compd. 2019;774(5):396–404. doi:10.1016/j.jallcom.2018.10.002.
2. Zhu XQ, Li WP, Li HL, Yuan JL, Qiao B, Zhou YX. Improvement of the DC electrical performance of silicone rubber for cable accessories through aromatic hydrocarbon voltage stabilizer. J Appl Polym Sci. 2022;139(20):52174. doi:10.1002/app.52174.
3. Ohki Y, Hirai N, Tanaka Y. Improvement of electrical insulation performance of silicone rubber cables due to exposure to heat and radiation. J Appl Polym Sci. 2023;140(43):e54595. doi:10.1002/app.54595.
4. Cherney EA. Silicone rubber dielectrics modified by inorganic fillers for outdoor high voltage insulation applications. IEEE Trans Dielectr Electr Insul. 2005;12(6):1108–15. doi:10.1109/TDEI.2005.1561790.
5. Kumara S. DC flashover characteristics of a polymeric insulator in presence of surface charges. IEEE Trans Dielectr Electr Insul. 2012;19(3):1084–90. doi:10.1109/TDEI.2012.6215116.
6. Imano AM. Accumulation of surface charges on the particle contaminated spacer surface in compressed gas under impulse voltage stress. J Electrostatics. 2004;61(1):1–19. doi:10.1016/j.elstat.2003.11.003.
7. Que LK, An ZL, Ma Y, Shan FT, Zhang YY, Zheng FH, et al. Improved DC flashover performance of epoxy insulators in SF6 gas by direct fluorination. IEEE Trans Dielectr Electr Insul. 2017;24(2):1153–61. doi:10.1109/TDEI.2017.006112.
8. Tseng JK, Tang S, Zhou Z, Mackey M, Carr JM, Mu R, et al. Interfacial polarization and layer thickness effect on electrical insulation in multilayered polysulfone/poly(vinylidene fluoride) films. Polymer. 2014;55(1):8–14. doi:10.1016/j.polymer.2013.11.042.
9. Zhou CL, Cao ZQ, Wei G, Wu K. Research on pyrolysis characteristics of PE outer sheath of high-voltage cables based on the principle of oxygen consumption. J Electr Eng Technol. 2023;18(1):679–85. doi:10.1007/s42835-022-01178-0.
10. Zhang YY, Li Y, Zheng HB, Zhu MZ, Liu JF, Yang T, et al. Microscopic reaction mechanism of the production of methanol during the thermal aging of cellulosic insulating paper. Cellulose. 2020;27(5):2455–67. doi:10.1007/s10570-019-02960-6.
11. Bamji SS, Bulinski AT, Densley RJ. Evidence of near-ultraviolet emission during electrical tree initiation in polyethylene. J Appl Phys. 1987;61(2):694–9. doi:10.1063/1.338221.
12. Gao Y, Wang M, Zhao N, Li Z, Liu Y, Han T, et al. Surface charge distribution measurement before and after DC flashover: a novel insight to the influence of surface charge on flashover voltage. In: Proceedings of the 2018 IEEE International Conference on High Voltage Engineering and Application (ICHVE); 2018 Sep 10–13; Athens, Greece. doi:10.1109/ICHVE.2018.8642199.
13. Han H, Gao C, Ding C, Qi B, Wang W, Li X, et al. Research on the suppression of nano-coatings for the surface charge accumulation on the GIS basin insulators under AC and DC voltage. In: Proceedings of the 2019 IEEE International Conference on Power, Intelligent Computing and Systems (ICPICS); 2019 Jul 12–14; Shenyang, China. doi:10.1109/ICPICS47731.2019.8942579.
14. Xie Q, Liang SD, Fu KX, Liu LZ, Huang H, Lv FC. Distribution of polymer surface charge under DC voltag and its influence on surface flashover characteristics. IEEE Trans Dielectr Electr Insul. 2018;25(6):2157–68. doi:10.1109/TDEI.2018.007268.
15. Wang F, Wen G, Fan F, Zhang T, Li J. Turn hydrophobic to superhydrophobic of composite insulators by surface fluorination. In: Proceedings of the 2016 IEEE International Conference on High Voltage Engineering and Application (ICHVE); 2016 Sep 19–22; Chengdu, China. doi:10.1109/ICHVE.2016.7800815.

16. Li S, Zhang RB, Wang SS, Fu YQ. Plasma treatment to improve the hydrophobicity of contaminated silicone rubber—the role of LMW siloxanes. IEEE Trans Dielectr Electr Insul. 2019;26(2):416–22. doi:10.1109/TDEI.2018.007732.
17. An ZL, Xie C, Jiang Y, Zheng FH, Zhang YW. Significant suppression of space charge injection into linear low density polyethylene by surface oxyfluorination. J Apply Phys. 2009;106(10):104112–4. doi:10.1063/1.3261847.
18. An ZL, Mao MJ, Yao JL, Zhang YW, Xia ZF. Fluorinated cellular polypropylene films with time-invariant excellent surface electret properties by post-treatments. J Phys D Appl Phys. 2010;43(41):415302. doi:10.1088/0022-3727/43/41/415302.
19. An ZL, Yang W, Xing ZL, Chen WJ, Chen K, Gao WJ, et al. Comparative study on direct fluorination and surface properties of alumina-filled and unfilled epoxy insulators. IEEE Trans Dielectr Electr Insul. 2020;27(1):85–93. doi:10.1109/TDEI.2019.008331.
20. An ZL, Qin YM, Chen TT, Xu JT. Further evidence and mechanisms for improvement in tracking and erosion resistance of ATH-free silicone rubbers by direct fluorination. IEEE Trans Dielectr Electr Insul. 2022;29(5):1685–92. doi:10.1109/TDEI.2022.3194493.
21. Lu T, Chen FW. Multiwfn: a multifunctional wavefunction analyzer. J Comput Chem. 2012;33(5):580–92. doi:10.1002/jcc.22885.
22. Christensen AS, Kubar T, Cui Q, Elstner M. Semiempirical quantum mechanical methods for noncovalent interactions for chemical and biochemical applications. Chem Rev. 2016;116(9):5301–37. doi:10.1021/acs.chemrev.5b00584.
23. Setianto S, Panatarani C, Singh D, Joni IM. Semi-empirical infrared spectra simulation of pyrene-like molecules insight for simple analysis of functionalization graphene quantum dots. Sci Rep. 2023;13(1):2282. doi:10.1038/s41598-023-29486-z.
24. Lu T, Chen FW. Quantitative analysis of molecular surface based on improved Marching Tetrahedra algorithm. J Mol Graph Model. 2012;38:314–23. doi:10.1016/j.jmgm.2012.07.004.
25. Humphrey W, Dalke A, Schulten K. VMD: visual molecular dynamics. J Mol Graph Model. 1996;14(1):33–8. doi:10.1016/0263-7855(96)00018-5.
26. Reynders JP, Jandrell IR, Reynders SM. Review of aging and recovery of silicone rubber insulation for outdoor use. IEEE Trans Dielectr Electr Insul. 2020;6(5):620–31. doi:10.1109/TDEI.1999.9286749.
27. Shen Z, An ZL, Chen T, Wang X, Zheng F, Zhang Y. Simultaneous improvement of surface properties of the liquid silicone rubber by direct fluorination. In: Proceedings of the 2020 IEEE 3rd International Conference on Dielectrics (ICD); 2020 Jul 5–31; Valencia, Spain. doi:10.1109/ICD46958.2020.9341879.
28. An ZL, Shen ZH, Gao WJ, Chen TT, Wang X, Zheng F, et al. Enhancement of DC flashover of liquid silicone rubber by direct fluorination. IEEE Trans Dielectr Electr Insul. 2020;27(6):2023–30. doi:10.1109/TDEI.2020.008860.
29. Chen TT, Shen ZH, An ZL, Zheng FH, Zhang YW. Effect of direct fluorination on tracking and erosion resistance of liquid silicone rubber. In: Proceedings of the 2020 IEEE International Conference on High Voltage Engineering and Application (ICHVE); 2020 Sep 6–10; Beijing, China. doi:10.1109/ICHVE49031.2020.9279762.
30. Okazawa K, Tsuji Y, Yoshizawa K. Understanding single-molecule parallel circuits on the basis of frontier orbital theory. J Phys Chem C. 2020;124(5):3322–31. doi:10.1021/acs.jpcc.9b08595.